*Knowledge-based Engineering and Sciences* (2022), **3**, (2), 18–35
doi:10.51526/kbes.2022.3.2.18-35

RESEARCH PAPER

# Flexural Behavior of Concrete-Filled Double-Skin Hexagonal Tubular Beams Using Finite Element Analysis

Zul Hakeem Bin Mazlana* and Ahmed W. Al Zand*

Civil Engineering Programme, Faculty of Engineering & Built Environment, Universiti Kebangsaan Malaysia, Malaysia
*Corresponding author. Email: a163680@ukm.edu.my; ahmedzand@ukm.edu.my

(Received 01 May 2022; revised 06 July 2022; accepted 01 August 2022; first published online 31 August 2022)

**Abstract**

The Concete-Filled Double Steel Tube (CFDST) members usually prepared from Concrete-Filled Steel Tube (CFST) member with additional internal steel tube, in order to increase strength and reduce the selfweight of the composite member. The conventional square cross-sections are usually used for the CFDST beams. However, these sectionsthis square section are usually facing an outward buckling failure at the compression zone stress that usually occurred at the top flange of the CFDST beams under high bending loads. Additionally, using cross-section shapes with hexagonal and/or octagonal and/or decagonal could be to reduce the flatness width of the CFDST beam's top flangem since they have smaller flatness width of their flanges than the square/rectangular tube's cross section. Therefore, the aim of this research is to numerically study the flexural behavior of CFDST beam with hexagonal tubular cross-section under pure bending static loads by using finite element (FE) software named ABAQUS. First, the FE model was devloped and verified with the rated experimental tested results, then devloped and analysed additional models of hexagonal CFDST beams to investigate further parameters that not yet been investiated. Generally a total of 19 hexagonal CFDST models were analysed for this project to investigate the influnce of varied tube's thickness ($t$), steel yielding strength ($f_y$), concrete strength ($f_{cu}$), inner to outer tube's dimensions ratio ($D_i/D_0$), and different inner tube's cross-sections shape (hexagon, square and circle). The result of the paper showed that by using double steel tube for the beam, the failure due to outward buckling can be reduced significantly. The ultimate bending capacity of the hexagon CFDST models were increased with increases of their steel/concrete strength, tube's thickness and $D_i/D_0$ ratio. For example, increasing the tube thickness from 1.5 mm 2.5 mm achieved an improvement in Mu values of about 41%. Meanwhile less improvement percentages was recorded when only the concrete strength increased. Furthermore, there are no much improvements have been recorded in the model's bending capacity when used square or circle shape of inner tube's cross-section the than the hexagonal shape. The energy absorption of the hexagon CFDST model have been improved according to the improvement of their loading strength capacities

**Keywords:** CFDST beam; outward buckling; flexural behaviour; finite element; modelling

## 1. Introduction

Generally, the Concrete Filled Double Skin Tubes (CFDST) member has almost all identical advantages as the Concrete-Filled Steel Tube (CFST) members, with better flexural stiffness and strength performance than the corresponding hollow steel tube [4, 12]. This innovative composite construction consists of two concentric steel tubes with concrete sandwiched between them. For example,

the outer steel tubes can be square hollow sections (SHS), while the inner tube can be the same shape square (SHS) or rectangular hollow sections (RHS) or even circular hollow section (CHS), also can be with several combinations and shapes. In recent years, the behavior of such CFDST columns has been studied by several researchers [9, 5]. The reviews indicate that almost all CFDST members studied in the literature were fabricated with circular steel tubes or square steel tubes. Only six preliminary tests on thin-walled rectangular CFDST stub columns were reported by [9], and not yet CFDST beam or beam-column with rectangular and hexagon sections was extensively investigated.

The behavior of thin-walled dodecagonal section CFDST beam-columns was studied by [3]. A series of test were carried out to measured deformation and strength to observe the section CFDSTs subjected to combined axial compression and flexural loading. The outer and inner tubes of the specimens were cold-formed steel dodecagonal hollow sections (DHS). The length of the specimen was set to 1998mm, 1999mm, 2000mm, 2001mm and 2002mm. The diameter of outer tube ranged from 399.5mm to 401.2mm with thickness of 2.99mm to 3.03mm. While the inner tube was set from 239.8mm to 240.3mm with the same range of thickness as the outer tube. In addition, FE model was developed using ABAQUS to examine the failure mode and the ultimate bearing capacity of tested specimens. Compressive force was applied at the top end of test specimens by hydraulic testing machine. Before the test begin, a small preload was applied to each specimen to examine the working performance of the test apparatus. For all test specimens, displacement control was used to move the hydraulic actuator at a constant speed. The use of displacement control made it possible to continue the experiments to the post-ultimate stage. During the experiments, a data acquisition system was used to monitor the applied load and the transducer readings at set intervals. Therefore, the result show that all the specimens tested showed good ductility. The diameter-to-thickness ratio of outer steel tubes has a major impact on dodecagonal section double skin concrete-filled steel tubes specimen behavior, whereas the diameter-to-thickness ratio of internal steel tubes appears to have a minor impact. The decreased of diameter-to-thickness ratio of outer steel tube cause the maximum axial load, load eccentricity and flexural stiffness of dodecagonal section double skin concrete-filled steel tubes to also decrease.

[3] also did a study on behavior of thin-walled dodecagonal section double skin concrete-filled steel tubes under bending. A finite element analysis and an experimental investigation were carried out in the study. studied in this paper. 7 beam specimens with length of 2000 mm were tested. The width to thickness ratio of the outer steel tube ranged from 75 to 133. The outer tube diameter was set at 300.2mm to 400.1mm with thickness of 2.98mm and 4.01mm. The inner diameter ranged from 179.7mm to 280mm and the thickness are 2.98mm, 2.99mm, 3.00mm, 3.01mm and 3.02mm. The load was slowly applied and monotonically increased until failure after some unloading and reloading cycles in the elastic domain. All the specimens undergo elastic stage, elastic–plastic stage and plastic stage during the test. No local buckling had occurred at the flat portion of outer steel tube in the compression zone and the specimens showed a good ductility.

In general, the CFDST beams usually prepared with conventional cross-sections [8, 14, 7]. However, these sections are usually facing an outward buckling failure at the compression zone stress that usually occurred at the top flange of the beams under high bending loads [11, 13]. Thus, using the outer tube's cross-section with irregular shapes such as hexagonal, octagonal, and decagonal shapes not yet extensively investigated. Additionally, using these irregular shapes could help to reduce the flatness width of the top flange, which delays the outward buckling that usually occurred at the CFST beam's top flange. In another word, the multi corners (6 corners) that provided for the hexagonal shape can stiffen the cross-section which expects to lead for better strength capacity compared to the equivalent square shape.

The objective of this paper is to observe the flexural behavior of concrete-filled double-skin hexagonal tubular beams using finite element analysis to develop and verified a finite element (FE) model of CFDST beams with an existing experimental tested specimen. and for further investigating

of paramters, including the effects of varied tube's thickness, and strengths of steel and concrete.

## 2. Methodology

### 2.1 Finite Element Model

The suggested FE models that developed in the current numerical study has been described in this section. Firstly, an experimental specimen that with rectangular shape cold-formed CFST beam was used to verify the developed FE model of this paper. Since there are no experimental works that investigated the CFDST beams with hexagonal shape, thus, the experimental results of CFST beam (SB1-C) that tested by [11] have been used to verify the control model of our current FE modelling study. The model is shown in Figure 1.

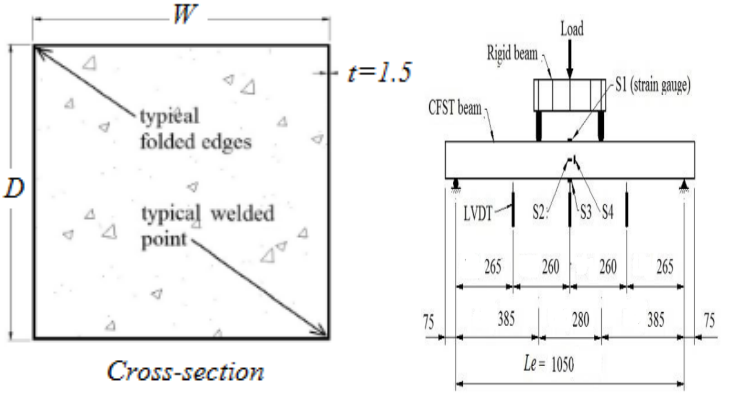


**Figure 1:** *The specimen SB1-C of CFST beam's cross-section ( Al Zand et al. 2020).*

Three different types of CFDST beam's cross-sections included the control sample were suggested for the current numerical investigation. The suggested hexagonal cross-sections of CFDST beams are presented in Figures 2 to 4. All these FE models are subjected to a pure flexural loading in order to simulating the actual beam that test by [11].

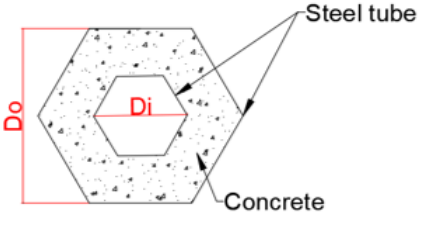


**Figure 2:** *Hexagonal CFDST with hexagonal inner tube.*

### 2.2 Parameter for FE model

The specimens' designations in the above tables are indicated the type of the studied CFDST models. For example, the "SB" refer to the Square Beam (control model that verified with experimental specimen SB1-C). The "HBH-G1-1" , the 1st letters "HBH" refer to the Hexagonal CFDST beam's model with Hexagonal inner tube, the 2nd letter "G1" refer to the Group number for studying the effects of tube's thickness (Table 1), lastly, the letter "1" refer to the 1st model's number in this group

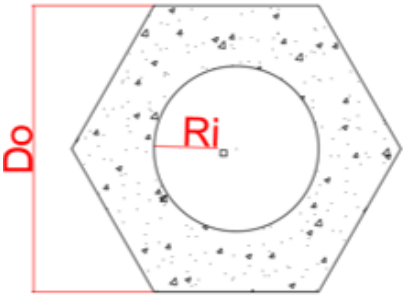


**Figure 3:** *Hexagonal CFDST with circular inner tube.*

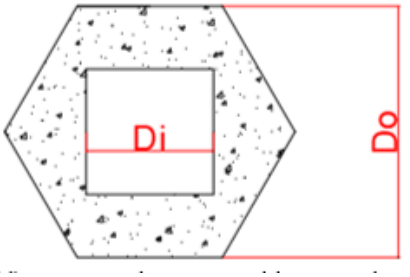


**Figure 4:** *Hexagonal CFDST with square inner tube.*

which is with $f_{cu}$ = 45.1 MPa, $f_y$ = 346 MPa, and $t$ = 1.5. The same numbering scenario was adopted for all FE models of CFDST beams that developed in this numerical study (Table 2 to Table 4). In addition, the "HBS" and "HBC" that provided in Table 5 (Group 5) are refers to Hexagonal CFDST beam's model with Square and Circular inner tube sections, respectively.

**Table 1:** *Hexagonal CFDST models with varied tube thickness – Group 1.*

| Specimen designation | Internal Tube | $f_{cu}$ (MPa) | $f_y$ (MPa) | t (mm) |
|---|---|---|---|---|
| SB | - | 45.1 | 346 | 1.5 |
| HBH-G1-1 | Hexagon | 45.1 | 346 | 1.5 |
| HBH-G1-2 | Hexagon | 45.1 | 346 | 2.0 |
| HBH-G1-3 | Hexagon | 45.1 | 346 | 2.5 |
| HBH-G1-4 | Hexagon | 45.1 | 346 | 3.0 |

**Table 2:** *Hexagonal CFDST models with varied tube strength – Group 2.*

| Specimen designation | Internal Tube | $f_{cu}$ (MPa) | $f_y$ (MPa) | t (mm) |
|---|---|---|---|---|
| SB | - | 45.1 | 346 | 1.5 |
| HBH-G2-1 | Hexagon | 45.1 | 346 | 1.5 |
| HBH-G2-2 | Hexagon | 45.1 | 250 | 1.5 |
| HBH-G2-3 | Hexagon | 45.1 | 450 | 1.5 |
| HBH-G2-4 | Hexagon | 45.1 | 550 | 1.5 |

**Table 3:** *Hexagonal CFDST models with varied concrete strength – Group 3.*

| Specimen designation | Internal Tube | $f_{cu}$ (MPa) | $f_y$ (MPa) | t (mm) |
|---|---|---|---|---|
| SB | - | 45.1 | 346 | 1.5 |
| HBH-G3-1 | Hexagon | 45.1 | 346 | 1.5 |
| HBH-G3-2 | Hexagon | 25.0 | 346 | 1.5 |
| HBH-G3-3 | Hexagon | 35.0 | 346 | 1.5 |
| HBH-G3-4 | Hexagon | 55.0 | 346 | 1.5 |

**Table 4:** *Hexagonal CFDST models with varied internal tube diameter – Group 4.*

| Specimen designation | Internal Tube | $f_{cu}$ (MPa) | $f_y$ (MPa) | $D_i/D_0$ ratio |
|---|---|---|---|---|
| SB | - | 45.1 | 346 | 0 |
| HBH-G4-1 | Hexagon | 45.1 | 346 | 0.5 |
| HBH-G4-2 | Hexagon | 45.1 | 346 | 0.6 |
| HBH-G4-3 | Hexagon | 45.1 | 346 | 0.7 |
| HBH-G4-4 | Hexagon | 45.1 | 346 | 0.8 |

**Table 5:** *Hexagonal CFDST models with varied internal tube shape – Group 5.*

| Specimen designation | Internal Tube | $f_{cu}$ (MPa) | $f_y$ (MPa) | t (mm) |
|---|---|---|---|---|
| SB | - | 45.1 | 346 | 1.5 |
| HBH-G5-1 | Hexagon | 45.1 | 346 | 1.5 |
| HBH-G5-2 | Hexagon | 25.0 | 346 | 1.5 |
| HBH-G5-3 | Hexagon | 35.0 | 346 | 1.5 |

### 2.3 Modelling Component

Figures 5 and 6 are presented the loading scenario and boundary conditions of the quarter 3D models of SB and HBH-G1-1 for example. Instead of using micro/macro muddling, full scale of 3D model has been built and analyzed which is the most concept used in the similar studies in the field of composite CFST and CFDST members as shown in the related references. The rolled supports are provided under the suggested FE models to simulate the actual scenario of the experimentally tested specimens, where the line of this support is allowed for rotate with no horizontal and vertical movement. The CFDST model is geometrically symmetric along the Z-Y and X-Y planes. Thus, only quarter model was developed and analysed to simulate the full model, following the same concept that adopted earlier in similar studies [15, 10, 2]. The downward displacement option that available in the ABAQUS software was used to representing the actual applied loads at the loading points shown in Figures 5 and 6, which these points were gradually moved downward during the FE analysis (much similar to the actual testing procedure in the lab).

### 2.4 Constitutive Model of Steel Tube

To identify the Young's modulus and the Poisson's ratio of steel tube are identified in the elastic-isotropic option that available in the ABAQUS software, while the yield strength and plastic strain values are identified in the option of plastic-isotropic. Figure 7 shows the trilinear stress–strain that used in the current FE model for the steel materials [11].

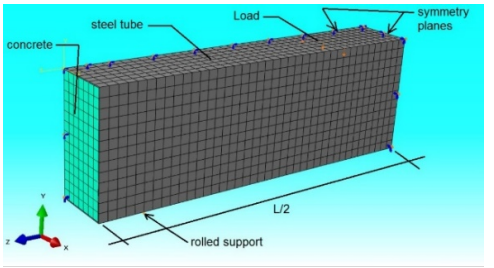


**Figure 5:** *Typical 3D FE model – quarter-model of SB.*

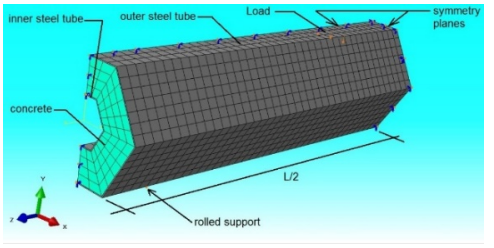


**Figure 6:** *Typical 3D FE model – quarter-model of HBH-G1-1.*

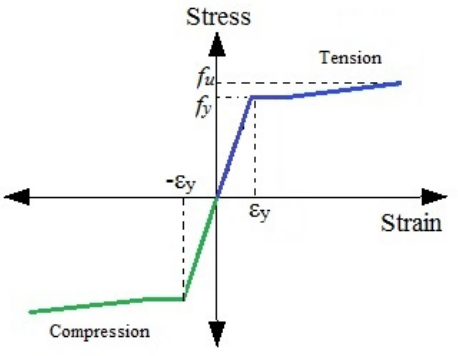


**Figure 7:** *Trilinear stress-strain relationships of steel tube in the FE model [11].*

### 2.5 Constitutive Model of Concrete

The compression and tension stresses are causing a crushing and cracking failures on the concrete material, since it is brittle material. Thus, in ABAQUS FE software, the modelling technique named 'Concrete Damage Plasticity' can derive these failures mechanisms by defining the 'Compressive Behaviour and Tensile Behaviour' of the concrete material (see Figure 8). This option was applied to similar FE study for the behaviour of infill concrete [11, 1]. From the software, the Poisson's ratio of concrete is 0.19 and the Young's modulus are predicted from Ec=4700. The strain at peak stress ($\epsilon_0$) were assumed to be 0.002 and the ultimate strain ($\epsilon_u$) were 0.0035 as adopted in similar FE studies [11, 6].

### 2.6 Elements Description

In ABAQUS/CAE there are several types of elements that can represent the parts of the suggested FE models. The model has different parameter that represent the CFDST beam which are outer

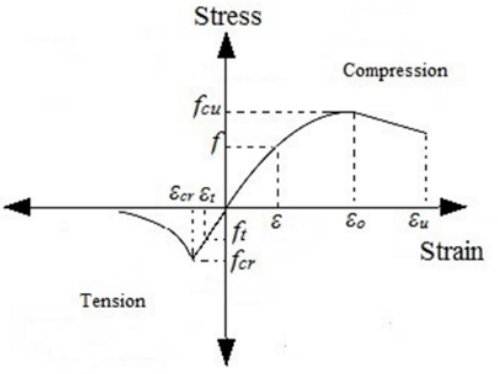


**Figure 8:** *Stress-strain relationships of concrete in the FE model [11].*

steel tube, concrete and internal tube. To model these materials, the element type of C3D8R were used for both of the concrete and steel tube parts, which is a 3D solid element with an eight-node linear brick, reduced integration and hourglass control [11]. For this element type, each node uses bilinear interpolation and has six degrees of freedom. Related shear-locking problems can be solved using the full integration of linear elements when subjected to bending loads. The element shows a highly stiff behavior in the bending process during this period. However, fully integrated linear elements only can be used when a small bending observed in the model.

### 2.7 Surface Interactions Description

The most important parameters for verifying the suggested FE models are the interaction among the surface of the CFST beam. ABAQUS can simulate the mechanical surface interactions between two deformable bodies which are steel tube and infill concrete by using the contact interaction option. The contact interaction is defined as two phases which are geometric and mechanical properties. The friction coefficient value can be affected by several parameters such as the type of infill concrete, the tube dimensions and the loading type/rate. All the CFDST models that developed in this research are used friction coefficient of 0.8, which is suggested based on several preliminary analyses investigation.

### 2.8 Convergence study

Based on the suggested modeling approach, the convergence study is one of the nonlinear solution procedures that achieve more accuracy of numerical solution, accuracy of time integration, accuracy of contact control and mesh convergence. The input parameters are defined and modeled before the investigation on the mesh convergence. A suitable-refined FE mesh will be used to achieve accurate results. A longer computational time in normal PCs are usually occurred when increase the number of elements but can achieve more accurate results. The converged solution for the FE model is considered by limit of meshing size/number of elements with the best and accurate results. Figure 9 illustrates the current convergence study on the relationship between the ultimate moment (Mu) value and the total number of elements used for the quarter FE models (SB).

## 3. Results and Discussion

### 3.1 Verification of Finite Element Model

The results obtain from the FE analysis are verified using the experimental result by [11]. Since there are no experimental works that investigated the CFDST beams with hexagonal shape, thus, the experimental results of square CFST beam (SB1-C) have been used to verify the control model

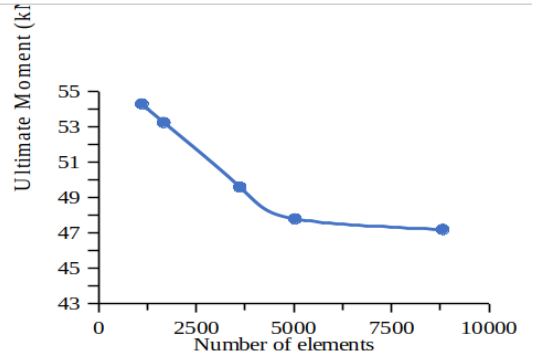


**Figure 9:** *Convergence study for the adopted total number of elements - 3D model.*

of our current FE modelling study. The same materials properties of this specimen were used to the develop FE model for current verification study. The result of the FE model was compared with the experimental result.

Figure 10 shows the moment vs. mid-span deflection relationships of the experimental specimen SB (SB1-C; tested by [11]. At the maximum deflection limit which is of about 26.6 mm (Le/40), The suggested FE mode SB was achieved ultimate bending value equal to 47.2 kN.m which is of about 4.2% higher that obtained from the corresponding specimen (45.3 kN.m) as compared in Table 6. In addition, bending behaviour including the buckling failure that occurred at the top flange of the tested specimen has been numerically simulated by the related FE mode, as shown in Figure 11.

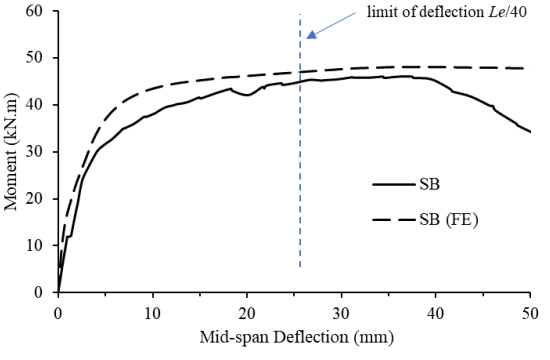


**Figure 10:** *10 Moment (kNm) vs Mid-span Deflection for SB.*

**Table 6:** *Hexagonal CFDST models with varied internal tube shape – Group 5.*

| Model ID | Mu (kN.m) | Load (kN) |
|---|---|---|
| SB | 45.3 | 259.1 |
| SB (FE) | 47.2 | 269.5 |

## 3.2 Parametric Studies

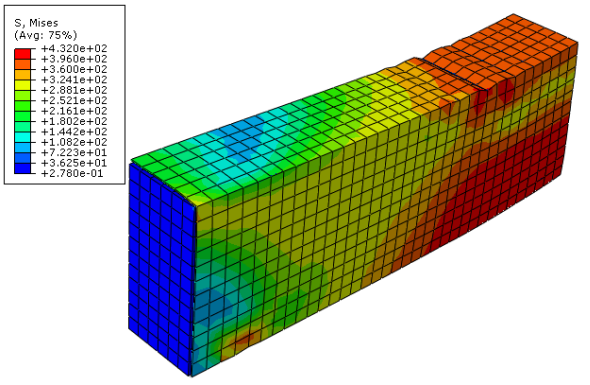


**Figure 11:** *Failure mode of the control FE model, SB.*

### *Effects of Tube Thickness (G1)*

The comparison between the moment vs. mid-span deflection of the analyzed models in G1 are shown in Figure 12, and the ultimate moment capacities (Mu) are compared in Figure 13. Table 7 show the result for this parameter.

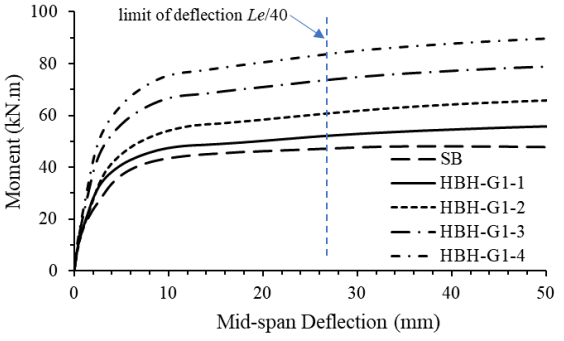


**Figure 12:** *Moment (kN.m) vs Mid-span deflection.*

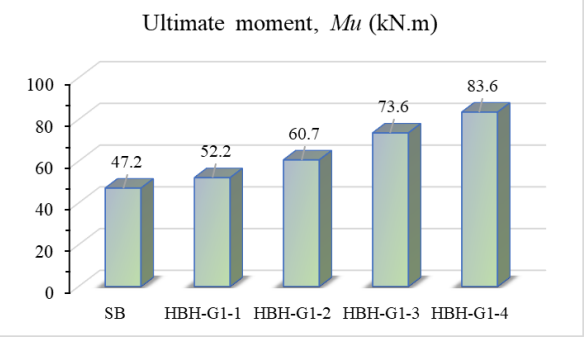


**Figure 13:** *Ultimate moment, Mu (kN.m).*

**Table 7:** *Effect of tube thickness on CFDST models in G1.*

| Model ID | Ultimate moment of parametric model (kN.m) | Percentage increase (%) |
|---|---|---|
| SB | 47.2 | - |
| HBH-G1-1 | 52.2 | - |
| HBH-G1-2 | 60.7 | 16.3 |
| HBH-G1-3 | 73.6 | 41.0 |
| HBH-G1-4 | 83.6 | 60.1 |

### *Effects of Tube Strength (G2)*

The steel yielding of the control model is 346 MPa. The first model for this group has the same steel yielding with the control model. The second model has lower value compared to the first model which is 250MPa. The steel yielding for the third and fourth model are 450MPa and 550Mpa. Figures 14 and 15 portrayed the data obtained from the model. The comparison value was presented in Table 8.

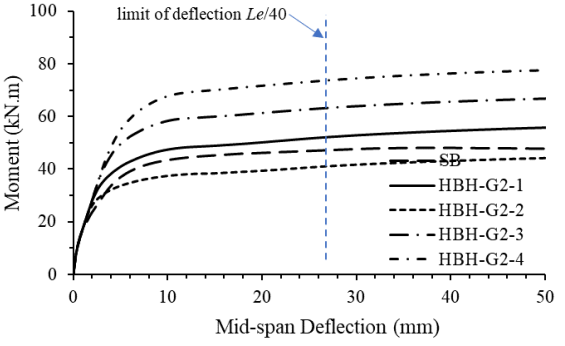


**Figure 14:** *Moment (kNm) vs Mid-span deflection.*

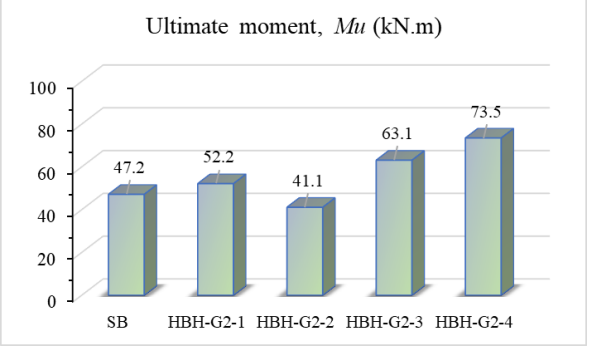


**Figure 15:** *Ultimate moment, Mu (kN.m).*

### *Effects of Concrete Strength (G3)*

This effect of concrete strength on the performance of the model was studied in this section. The control model and the first model both have 45.1MPa for the concrete strength. The concrete

**Table 8:** *Effect of tube thickness on CFDST models in G1.*

| Model ID | Ultimate moment of parametric model (kN.m) | Percentage increase (%) |
|---|---|---|
| SB | 47.2 | - |
| HBH-G3-1 | 52.2 | - |
| HBH-G3-2 | 48.7 | -6.7 |
| HBH-G3-3 | 53.0 | 1.6 |
| HBH-G3-4 | 55.1 | 5.6 |

strengths in this parameter are 25.0MPa, 35.0Mpa and 55.0MPa for model 2, model 3 and model 4 respectively. The results are showed in Figures 16 and 17. Table 9 show the result for this parameter.

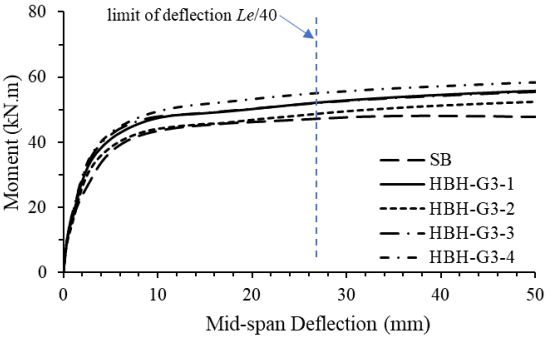


**Figure 16:** *Moment (kNm) vs Mid-span deflection.*

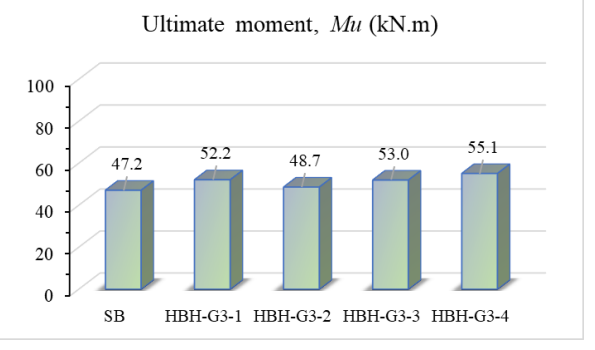


**Figure 17:** *Ultimate moment, Mu (kN.m).*

### *Effects of Internal Steel Tube Diameter (G4)*

The diameter of internal steel tube was observed for the next variable. The effect of internal steel tube with different diameter on the model was studied. The control model did not have any internal tube. The first model has the ratio of 0.5 for internal diameter to outside diameter. The model 2, model 3 and model 4 has the internal diameter to outside diameter ratio of 0.6, 0.7 and 0.8. Figures 18 and 19 present the results obtained from the model Table 10 show the result for this parameter.

**Table 9:** *Effect of concrete strength on CFDST.*

| Model ID | Ultimate moment of parametric model (kN.m) | Percentage increase (%) |
|---|---|---|
| SB | 47.2 | - |
| HBH-G3-1 | 52.2 | - |
| HBH-G3-2 | 48.7 | -6.7 |
| HBH-G3-3 | 53.0 | 1.6 |
| HBH-G3-4 | 55.1 | 5.6 |

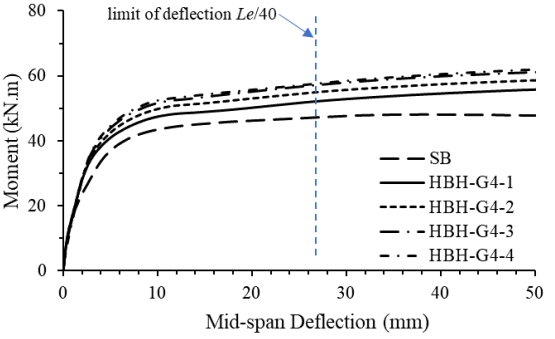


**Figure 18:** *Moment (kNm) vs Mid-span deflection.*

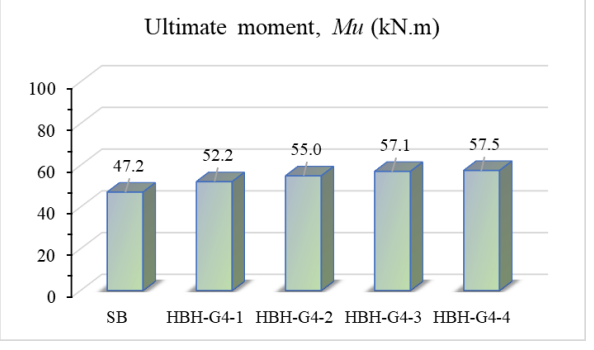


**Figure 19:** *Ultimate moment, Mu (kN.m).*

**Table 10:** *Effect of internal steel tube diameter on CFDST.*

| Model ID | Ultimate moment of parametric model (kN.m) | Percentage increase (%) |
|---|---|---|
| SB | 47.2 | - |
| HBH-G4-1 | 52.2 | - |
| HBH-G4-2 | 55.0 | 5.3 |
| HBH-G4-3 | 57.1 | 9.3 |
| HBH-G4-4 | 57.5 | 10.1 |

### *Effects of Internal Steel Tube Shape (G5)*

The last parameter that was observed is CFDST with different internal steel tube shape. Just like the previous parameters studied, the control model does not have internal tube. The internal tube shape

consisted of hexagon for model 1, square for model 2 and circle for model 3. The result was shown in Figures 20 and 21. Table 11 show the result for this parameter.

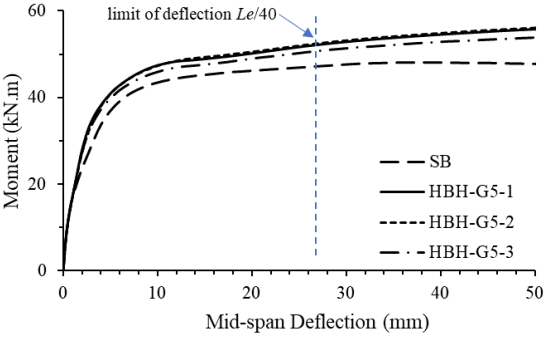


**Figure 20:** *Moment (kNm) vs Mid-span deflection.*

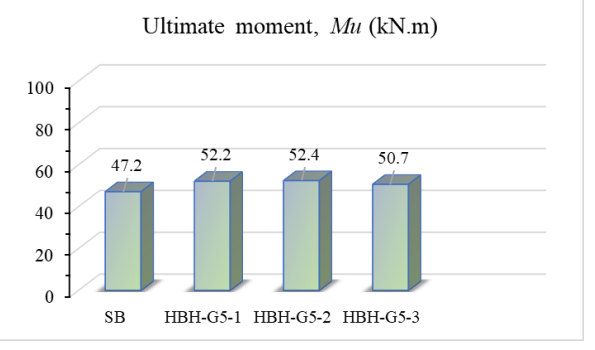


**Figure 21:** *Ultimate moment, Mu (kN.m).*

**Table 11:** *Effect of internal steel tube shape on CFDST.*

| Model ID | Ultimate moment of parametric model (kN.m) | Percentage increase (%) |
|---|---|---|
| HBH-G5-1 | 52.2 | - |
| HBH-G5-2 | 52.4 | 0.3 |
| HBH-G5-3 | 50.7 | -2.8 |

### 3.3 Energy Absorption

In this section, the energy absorption (EA) by the hexagonal CFDST model were discussed. The EA of the model was observed from the area under the load. The EA were obtained based on the load deflection curved of the respective group.

#### *Effects of Tube Thickness (G1)*

The EA are corresponded to the performance of the CFDST model. The results were presented in Figure 22 and Table 12. HBH-G1-1 achieved EA value equal to 6,915 kN.mm, which is higher than that of the square control model SB with an improvement of about 10.8%, even when both of them

have 1.5 mm outer tube's thickness. Additionally, the EA value of the same HBH-G1 model increased up 10,806 kN.mm when only the tube's thickness increase to 3.0 mm, achieving an improvement of about 56.2%, compared to the value of HBH-G1 model.

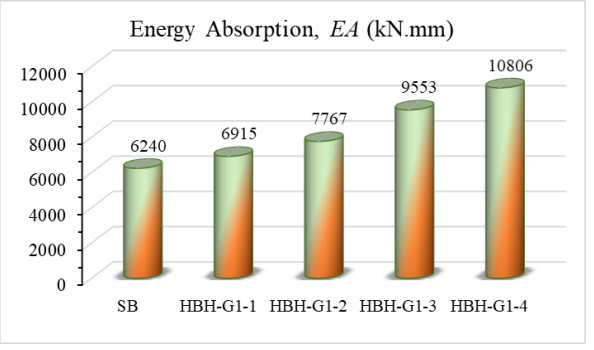


**Figure 22:** *Energy Absorption of G1.*

**Table 12:** *EA values for models in G1.*

| Model ID | Energy absorption of parametric model (kN.mm) | Percentage increase (%) |
|---|---|---|
| SB | 6,240 | - |
| HBH-G1-1 | 6,915 | - |
| HBH-G1-2 | 7,767 | 12.3 |
| HBH-G1-3 | 9,553 | 38.1 |
| HBH-G1-4 | 10,806 | 56.2 |

### *Effects of Tube Strength (G2)*

The EA of HBH-G-2 is the lowest compared to other models in this group due to having lower tube strength. The strength of the tube is heavily affected by the steel itself. Having lower strength will reflect the poorly on the performance of the model. The results were showed in Figure 23 and Table 13.

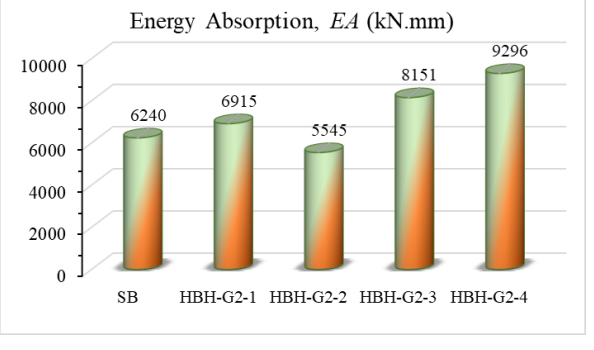


**Figure 23:** *Energy Absorption of G2.*

**Table 13:** *EA values for models in G2.*

| Model ID | Energy absorption of parametric model (kN.mm) | Percentage increase (%) |
|---|---|---|
| SB | 6,240 | - |
| HBH-G2-1 | 6,915 | - |
| HBH-G2-2 | 5,545 | -19.8 |
| HBH-G2-3 | 8,151 | 17.8 |
| HBH-G2-4 | 9,296 | 34.4 |

### *Effects of Concrete Strength (G3)*

Even with lower concrete strength, HBH-G3-2 still has higher EA compared the control model. Inner steel tube improved the EA and overall performance of the CFDST. The results were presented in Figure 24 and Table 14.

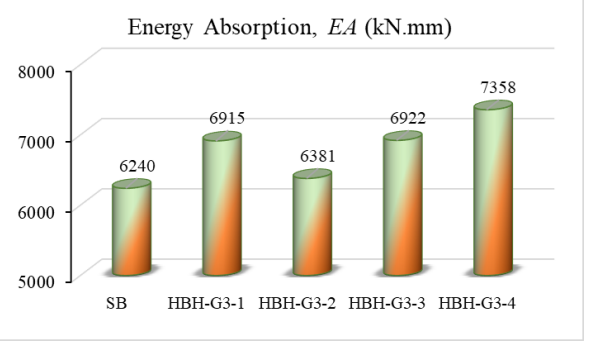


**Figure 24:** *Energy Absorption of G3.*

**Table 14:** *EA values for models in G3.*

| Model ID | Energy absorption of parametric model (kN.mm) | Percentage increase (%) |
|---|---|---|
| SB | 6,240 | - |
| HBH-G3-1 | 6,915 | - |
| HBH-G3-2 | 6,381 | -0.77 |
| HBH-G3-3 | 6,922 | 0.1 |
| HBH-G3-4 | 7,358 | 6.4 |

### *Effects of Internal Steel Tube Diameter (G4)*

The CFDST with bigger internal tube diameter have higher EA. Despite having different diameter for each model, the EA are relatively similar to each other. The results were presented in Figure 25 and Table 15.

### *Effects of Internal Steel Tube Shape (G5)*

The changes in inner steel tube shapes does not having significant impact on the EA of CFDST. HBH -G5-3 has the lowest EA among the CFDST in this group. But it still has higher EA compared to the control model. The results were showed in Figure 26 and Table 16.

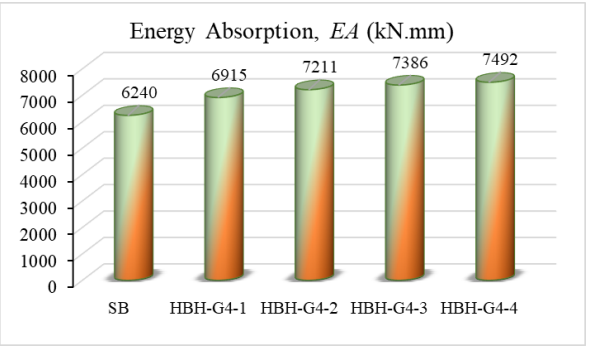


**Figure 25:** *Energy Absorption of G4.*

**Table 15:** *EA values for models in G4.*

| Model ID | Energy absorption of parametric model (kN.mm) | Percentage increase (%) |
|---|---|---|
| SB | 6,240 | - |
| HBH-G4-1 | 6,915 | - |
| HBH-G4-2 | 7,211 | 4.3 |
| HBH-G4-3 | 7,386 | 6.8 |
| HBH-G4-4 | 7,492 | 8.3 |

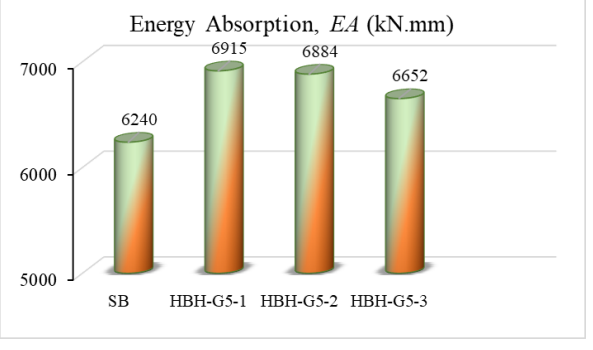


**Figure 26:** *Energy Absorption of G5.*

**Table 16:** *EA values for models in G5.*

| Model ID | Energy absorption of parametric model (kN.mm) | Percentage increase (%) |
|---|---|---|
| SB | 6,240 | - |
| HBH-G5-1 | 6,915 | - |
| HBH-G5-2 | 6,884 | -0.4 |
| HBH-G5-3 | 6,652 | -3.3 |

## 4. Conclusion

This paper involves finite element (FE) analyses of hexagonal cncrete-filled double-skin steel tube (CFDST) beam that are subjected to pure flexural loading. The analysis was carried out by using ABAQUS software to investigate the flexural performance of CFDST models. The experimental

results of CFST beam that are experimentally tested by [11] was used as reference for verifying the currently developed CFST model. After that, a total 19 hexagonal CFDST models were developed and analysed to investigate the effects of different parameters. These FE models were divided into 5 group which are stated in Chapter III. First group (G1) have four model with different tube thickness for the outer tubes. For the second group (G2), the tube strength was varied for four models. The four models in the third group (G3) have different concrete strength. The internal tube diameter was varied for four models in the fourth group (G4). Lastly the fifth group (G5) have different internal tube shapes. The conclusions of the current numerical analyses are summarized as follows:

- First, the validity of the suggested FE model has been confirmed, where the developed and analysed CFST model was slightly overestimated the bending capacity of the corresponding tested specimen with of about 4%. In addition, the flexural performance including the failure mode of the CFST model were adequately achieved the experimental one.
- Increasing the outer tube thickness led to increase the hexagon CFDST model's bending capacity accordingly, where increasing the t value from 1.5mm to 2.5mm and 3.0mm, increased the Mu value of about 41% and 60.1%, respectively.
- Increasing the tube's yielding strength led to increase the hexagon CFDST model's capacity as well. For example, the Mu value increased of about 20.8% and 40.8%, when only the $f_y$ value increased from 346 MPa to 450 MPa and 550 MPa, respectively.
- Similar performance was recorded when the concrete strength of the infill material was increased but with limited improvement percentages. For example, increasing only the $f_{cu}$ value of the hexagon CFDST model from 25 MPa to 55 MPa increased the Mu value from 48.7 kN.m to 55.1 kN.m (+13.14%).
- Increasing the inner tube diameter ($D_i/D_0$ ratio) led to increase the Mu value of the hexagon CFDST model, where increasing the $D_i/D_0$ ratio from 0.5 to 0.8 let to increase the Mu value of about 10.1%.
- Moreover, adopting different internal tube cros–section than the hexagonal shape does not have limited impact to the ultimate capacity of the investigated hexagon CFDST model. For example, the model's strength capacity canged of about +0.3% and -2.8% when only change the inner tube section from hexagon to square and circle shape, respectively, with keeping the same $D_i/D_0$ ratio.
- Finally, the energy absorption index of the hexagonal CFDST models was improved due to the improvement of their tube's thickness/strength, concrete strength values and $D_i/D_0$ ratio. However, using different inner tube's shape than the hexagonal shape doesn't led to improve the energy absorption index of the investigated CFDST model

The currently investigated FE models are limited to the hexagonal cross-section, concrete strength up to 55 MPa, steel yield strength up to 550 MPa, tube thickness up to 3 mm, and length-to-depth ratio is 5.25. Therefore, in order to more understand the structural behaviors of the CFDST members with unconventional cross-section, then further numerical analyses are recommended for investigate the influence of varied cross section than the hexagon shape and consider different stress-strain relationships of the concrete/steel/stainless steel materials, boundary conditions and loading scenarios.

**Conflicts of Interest:** **The authors have no conflict of interest to any part.**

## References


[1] A. A. Abdulhameed et al. "The behavior of hybrid fiber-reinforced Concrete Elements: A new stress-strain model using an evolutionary approach". In: *Appl. Sci.* 12.4 (2022), p. 2245.

[2] M. I. Alam and S. Fawzia. "Numerical studies on CFRP strengthened steel columns under transverse impact". In: *Compos. Struct.* 120 (2015), pp. 428–441.

[3] J. Chen et al. "Behavior of thin-walled dodecagonal section double skin concrete-filled steel tubular beam-columns". In: *Thin-Walled Struct.* 104 (2016), pp. 135–143.

[4] N. M. R. Dabbagh et al. "A systematic review on CFST members under impulsive loading". In: *Thin-Walled Struct.* 179 (2022), p. 109503.

[5] L. H. Han, C. C. Hou, and W. Xu. "Seismic performance of concrete-encased column base for hexagonal concrete-filled steel tube: numerical study". In: *J. Constr. Steel Res.* 149 (2018), pp. 225–238.

[6] S. J. Hilo et al. "Structural behavior of composite wall systems strengthened with embedded cold-formed steel tube". In: *Thin-Walled Struct.* 98 (2016), pp. 607–616.

[7] S. J. Lee. "An experimental study on concrete-filled double-skin square steel tubular beams under a concentrated load". In: *JAIK* 38.2 (2022), pp. 169–176.

[8] W. Li et al. "Performance of CFDST beams using high-strength steel under bending". In: *Structures.* 34 (2021), pp. 2644–2655.

[9] Z. Tao and L. H. Han. "ehaviour of concrete-filled double skin rectangular steel tubular beam-columns". In: *J. Constr. Steel Res.* 62.7 (2006), pp. 631–646.

[10] A. W. Al-Zand et al. "Finite element analysis of square CFST beam strengthened by CFRP composite material". In: *Thin-Walled Struct.* 96 (2015), pp. 348–358.

[11] A. W. Al-Zand et al. "Flexural performance of square concrete-filled steel tube beams stiffened with V-shaped grooves". In: *J. Constr. Steel Res.* 166 (2020), p. 105930.

[12] A. W. Al-Zand et al. "Performance of the novel C-purlin tubular beams filled with recycled-lightweight concrete strengthened with CFRP sheet". In: *J. Build. Eng.* 43 (2021), p. 102532.

[13] A. W. Al-Zand et al. "Stiffening performance of cold-formed C-section beam filled with lightweight-recycled concrete mixture." In: *Materials* 15.9 (2022), p. 2982.

[14] Z. Zhang et al. "Concrete-filled double steel tubular beams under lateral impact". In: *Case Stud. Constr. Mater.* (2022), e01252.

[15] H. Al-Zubaidy, X. L. Zhao, and R. Al-Mahaidi. "Mechanical characterisation of the dynamic tensile properties of CFRP sheet and adhesive at medium strain rates". In: *Compos. Struct.* 96 (2013), pp. 153–164.